Dynamics and Control of Direct-Drive Robots with Positive Joint Torque Feedback

F. Aghili and M. Buehler

Dept. Mechanical Engineering
McGill University
Montréal, QC H3A 2A7, Canada

J. M. Hollerbach

Dept. Computer Science
University of Utah
Salt Lake City, UT 84112, USA

Abstract

This paper addresses the dynamics and control of direct drive robots with positive joint torque feedback. We analytically derive the system dynamics in closed form. Even though it is coupled and nonlinear in general, it is substantially simpler than the robot link dynamics. We also derive conditions on the robot configuration which result in linear dynamics. Motion control laws for both cases are proposed.

1 Introduction

Direct drive motors simplify greatly the mechanical complexity of actuated joints by eliminating the transmission systems required with traditional electric actuators. In addition they permit accurate torque control at each joint, through eliminating backlash, compliance, and much of the friction incurred with gear transmissions [2, 3]. These properties are leading to an increasing popularity of direct drive motors in robots and manufacturing systems. In an effort to improve upon the torque-to-mass ratio and torque accuracy of previous designs, a new direct drive 3-phase synchronous motor, the McGill/MIT Direct Drive Motor, has been designed and constructed [9]. Our work on motor control with positive joint torque feedback is based on this actuator.

The production of accurate torque, however, is complicated by the nonlinearity of the motor itself. The control problem of how to translate a desired torque command faithfully into a motor torque and the underlying motor model have been studied by several researchers [13, 17, 6, 4, 16]. In [1], we proposed an indirect adaptive control strategy for the McGill/MIT Direct Drive Motor. Once accurate torque production is achieved, accurate and high bandwidth control of direct drive robots still requires the compensation of the nonlinear link dynamics. Linearization methods can be applied, like nonlinear decoupling control [7], resolved acceleration control [12], or the computed torque method [2, 15]. These approaches depend on the precise knowledge of the robot parameters and of the possibly varying load, and perform poorly when the model is not accurate [2, 18].

We focus on the case where the actuator can provide precise driving torque without the need for torque sensor feedback. Now joint torque measurements can be used for *positive* feedback to compensate the effects of the manipulator dynamics. For this purpose we have designed and built a new torque sensor which has been optimized via finite elements for high stiffness, low torsional sensitivity, and low sensitivity to non-torsional forces. The system dynamics are determined completely by the motion of the motor rotors in the Cartesian space which is not detectable by the torque sensors. Kosuge [11] demonstrated experimentally the effectiveness of using joint torque measurements to compensate the nonlinear link dynamics of a SCARA-type direct drive robot. However, he noticed a torque disturbance on the rotors caused by the movement of the proximal joints, which is not detectable by the torque sensors. Hashimoto [8] applied this technique to a harmonic drive actuator where the deformation of the "flex-spline" is used to measure joint torque. He claimed that the dynamic coupling terms in the robot dynamics are small due to the high angular velocity of the rotors in comparison to that of the links, and therefore can be treated as disturbances.

In this paper we present the general derivation of the Lagrangian for direct drive robots with joint torque feedback in closed form. The only parameters needed are the polar inertias of the rotors and the twist angles between adjacent joint axes. The next section is devoted to designing the outer loop control law depending on the robot's kinematic configuration. First, we derive the condition on the robot configuration resulting in a linear multi-input system which facilitates the control problem. For the nonlinear case, feedback linearization or equivalently inverse dynamics should be employed to linearize the system. The detail design of the whole control law is presented for a general three DOF robot.

2 Robot Dynamics with Positive Joint Torque Feedback

We investigate robots which are open kinematic chains with revolute joints where each joint is instrumented with a torque sensor. Fig. 1 depicts the ith joint of a such robot where the torque sensor is located between motor shaft and the next link. To apply the Lagrangian methodology, we cut the motor shaft right at the location of the torque sensor. By this means we add a virtual joint at each robot joint. Suppose $\boldsymbol{\theta}, \boldsymbol{\phi} \in \mathbb{R}^n$ are the link and drive angle vector respectively, while $\boldsymbol{\phi} \equiv \boldsymbol{\theta}$, if the torque sensor compliance is neglected.

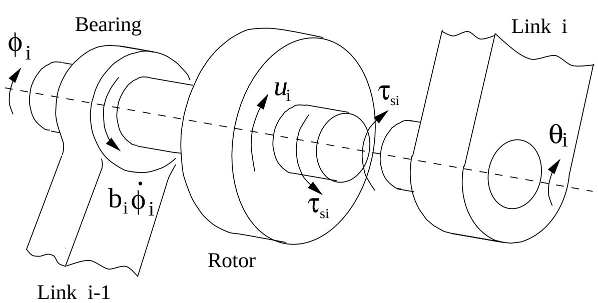

Figure 1: ith robot joint.

Let $\mathbf{z}_j^i$ be a unit vector in the direction of the jth joint axis expressed in the frame attached to the ith joint, consistent with Craig's notation [5]. Then

$$\mathbf{z}_j^i(\boldsymbol{\theta}) = \mathbf{R}_j^i(\boldsymbol{\theta})\hat{\mathbf{k}},$$

where $\hat{\mathbf{k}} = [0,0,1]^T$ and $\mathbf{R}_j^i(\boldsymbol{\theta})$ is the homogeneous rotation transformation [3],

$$\mathbf{R}_j^i = \prod_{q=j}^{i-1} \mathbf{R}_q^{q+1}$$

and

$$\mathbf{R}_q^{q+1} = \begin{bmatrix} c\theta_{q+1} & s\theta_{q+1}c\alpha_q & s\theta_{q+1}s\alpha_q \\ -s\theta_{q+1} & c\theta_{q+1}c\alpha_q & c\theta_{q+1}s\alpha_q \\ 0 & -s\alpha_q & c\alpha_q \end{bmatrix}. \quad (1)$$

Here $\sin\theta_q$ and $\cos\theta_q$ are represented by $s\theta_q$ and $c\theta_q$ for brevity. With these definitions we can express the absolute linear and angular velocities in various frames,

$$\boldsymbol{\omega}_i^i = \sum_{j=1}^{i} \mathbf{z}_j^i(\boldsymbol{\theta})\dot{\theta}_j, \quad \boldsymbol{\Omega}_i^i = \sum_{j=1}^{i-1} \mathbf{z}_j^i(\boldsymbol{\theta})\dot{\theta}_j + \dot{\phi}_i\hat{\mathbf{k}}, \quad (2)$$

$$\mathbf{v}_{ci} = \sum_{j=1}^{i-1}(\mathbf{z}_j^i(\boldsymbol{\theta})\dot{\theta}_j \times \mathbf{r}_{j,ci}) + \dot{\phi}_i\hat{\mathbf{k}} \times \mathbf{r}_{i,ci}, \quad (3)$$

where $\boldsymbol{\omega}_i^i$ and $\boldsymbol{\Omega}_i^i$ are the corresponding rotor and link angular velocities, $\mathbf{r}_{j,ci}$ is a vector from any point on the jth axis to the centroid of ith rotor and $\mathbf{v}_{ci}$ is the linear velocity of this rotor, all expressed in the frame of the ith joint. In practice, rotors are statically balanced, and the principal axes of all rotor inertias lie on the joint axes. Thus $\mathbf{r}_{i,ci}$ is collinear with $\hat{\mathbf{k}}$, and consequently the last term in (3) is zero. The total kinetic energy of the robot is distributed in its links, associated with link inertia $\mathbf{M}_L$, and its rotors. Now, given the inertia matrix of the ith rotor as,

$$\mathbf{J}^{(i)} = \begin{bmatrix} J_{xx}^{(i)} & 0 & 0 \\ 0 & J_{yy}^{(i)} & 0 \\ 0 & 0 & J_{zz}^{(i)} \end{bmatrix},$$

and its mass m_i, the kinetic energy of the rotors is

$$T = \frac{1}{2}\dot{\boldsymbol{\theta}}^T\mathbf{M}_L(\boldsymbol{\theta})\dot{\boldsymbol{\theta}} + \frac{1}{2}\sum_{i=1}^{n} m_i\mathbf{v}_{ci}^T\mathbf{v}_{ci} + \frac{1}{2}\sum_{i=1}^{n}\boldsymbol{\Omega}_i^T\mathbf{J}^{(i)}\boldsymbol{\Omega}_i.$$

Substituting for $\mathbf{v}_{ci}$, $\boldsymbol{\omega}_i$ and $\boldsymbol{\Omega}_i$ from (2) and (3) and expanding the relevant terms yields the kinetic energy as a quadratic function of $\dot{\boldsymbol{\theta}}$ and $\dot{\boldsymbol{\phi}}$. The $\dot{\boldsymbol{\theta}}$ dependent terms are caused by $\mathbf{M}_L$, angular velocity from (2) say $\mathbf{M}_{\dot{\boldsymbol{\phi}}}$ and linear velocity from (3) say $\mathbf{M}_v$. Hence we have

$$T = \frac{1}{2}\dot{\boldsymbol{\theta}}^T\mathbf{M}_T(\boldsymbol{\theta})\dot{\boldsymbol{\theta}} + \frac{1}{2}\dot{\boldsymbol{\phi}}^T\mathbf{J}_p\dot{\boldsymbol{\phi}} + \dot{\boldsymbol{\theta}}^T\mathbf{D}(\boldsymbol{\theta})\mathbf{J}_p\dot{\boldsymbol{\phi}} \quad (4)$$

where

$$\mathbf{M}_T(\boldsymbol{\theta}) = \mathbf{M}_L(\boldsymbol{\theta}) + \mathbf{M}_v(\boldsymbol{\theta}) + \mathbf{M}_{\dot{\boldsymbol{\phi}}}(\boldsymbol{\theta})$$

is that part of the robot kinetic energy which depends only on $\dot{\boldsymbol{\theta}}$. Since the robot kinetic energy is equal to the first term in (4) when $\dot{\boldsymbol{\phi}} = 0$, $\mathbf{M}_T(\boldsymbol{\theta})$ can be interpreted as inertia of a robot when the ith rotor is "locked" to the $(i-1)$th link. $\mathbf{J}_p$ is a diagonal matrix whose diagonal elements contain the z-axis components of the rotor inertias which are shown hereafter with J_i for convenience of notation, $\mathbf{J}_p = \mathrm{diag}[J_1, J_2, ..., J_n]$. The "configuration matrix" $\mathbf{D}(\boldsymbol{\theta})$ is a strictly upper triangle matrix

$$\mathbf{D}(\boldsymbol{\theta}) \stackrel{def}{=} \begin{bmatrix} 0 & \hat{z}_1^2 & \hat{z}_1^3(\boldsymbol{\theta}) & \hat{z}_1^4(\boldsymbol{\theta}) & \cdots & \hat{z}_1^n(\boldsymbol{\theta}) \\ 0 & 0 & \hat{z}_2^3 & \hat{z}_2^4(\boldsymbol{\theta}) & \cdots & \hat{z}_2^n(\boldsymbol{\theta}) \\ 0 & 0 & 0 & \hat{z}_3^4 & \cdots & \hat{z}_3^n(\boldsymbol{\theta}) \\ \vdots & \vdots & \vdots & \vdots & \vdots & \vdots \\ 0 & 0 & 0 & 0 & \cdots & \hat{z}_{n-1}^n(\boldsymbol{\theta}) \\ 0 & 0 & 0 & 0 & \cdots & 0 \end{bmatrix}. \tag{5}$$

The $\hat{z}_j^i$ elements present the projection of jth joint axis on the ith one which turns out to be the $(3,3)$ element of the rotation matrix $\mathbf{R}_j^i(\boldsymbol{\theta})$,

$$\hat{z}_j^i = \mathbf{z}_j^i \cdot \hat{\mathbf{k}} = [\mathbf{R}_j^i(\boldsymbol{\theta})]_{(3,3)}.$$

The gravitational potential energy $V_g(\boldsymbol{\theta})$ is only a function of the joint angles $\boldsymbol{\theta}$ because the mass centre of each rotor lies on its joint axis. Now the Euler-Lagrange equation can be derived as

$$\begin{aligned} \mathcal{L} &= T - V = \frac{1}{2}\dot{\boldsymbol{\theta}}^T \mathbf{M}_T(\boldsymbol{\theta})\dot{\boldsymbol{\theta}} + \frac{1}{2}\dot{\boldsymbol{\phi}}^T \mathbf{J}_p \dot{\boldsymbol{\phi}} \\ &\quad + \dot{\boldsymbol{\theta}}^T \mathbf{D}(\boldsymbol{\theta}) \mathbf{J}_p \dot{\boldsymbol{\phi}} - \mathbf{V}_g(\boldsymbol{\theta}). \end{aligned} \tag{6}$$

From (7) the equations of motion are

$$\begin{aligned} \frac{d}{dt}\left(\frac{\partial \mathcal{L}}{\partial \dot{\boldsymbol{\theta}}}\right) - \frac{\partial \mathcal{L}}{\partial \boldsymbol{\theta}} &= \boldsymbol{\tau}_s, \\ \frac{d}{dt}\left(\frac{\partial \mathcal{L}}{\partial \dot{\boldsymbol{\phi}}}\right) - \frac{\partial \mathcal{L}}{\partial \boldsymbol{\phi}} &= \mathbf{u} - \boldsymbol{\tau}_s - \mathbf{B}\dot{\boldsymbol{\phi}}. \end{aligned}$$

The first equation yields the system equation of motion in terms of robot link parameters, whereas the second relies on that of the rotors. The right hand side shows the net torques acting on the joints, consisting of the driving torques $\mathbf{u}$, the external torques measured via $\boldsymbol{\tau_s}$, and the viscous friction torques. Since $\boldsymbol{\tau_s}$ is available in real time, after defining a new compensated input,

$$\bar{\mathbf{u}} = \mathbf{u} - \boldsymbol{\tau}_s, \tag{7}$$

and substituting $\boldsymbol{\phi}$ with $\boldsymbol{\theta}$, assuming rigid torque sensor, the rotor dynamics are

$$\mathbf{J}_p\ddot{\boldsymbol{\theta}} + \mathbf{B}\dot{\boldsymbol{\theta}} + \frac{d}{dt}\left(\mathbf{J}_p\mathbf{D}^T(\boldsymbol{\theta})\dot{\boldsymbol{\theta}}\right) = \bar{\mathbf{u}}.$$

Since $\hat{z}_j^i = \hat{z}_j^i(\theta_{i+1}, \theta_{i+2}, \cdots, \theta_j)$, we have,

$$\frac{d}{dt}\hat{z}_j^i = \sum_{r=i+1}^{j} \dot{\theta}_r \frac{\partial \hat{z}_j^i}{\partial \theta_r}.$$

Suppose $\mathbf{C}(\boldsymbol{\theta}, \dot{\boldsymbol{\theta}}) = \frac{D}{Dt}\mathbf{D}^T(\boldsymbol{\theta})$, then the matrix elements can be carried out as

$$c(j,i) = \begin{cases} \frac{d}{dt}\hat{z}_j^i & \text{if } j > i+1 \\ 0 & \text{otherwise.} \end{cases} \tag{8}$$

Finally, the system dynamics can be represented in the standard form as

$$\mathbf{J}_p\left(\mathbf{I} + \mathbf{D}^T(\boldsymbol{\theta})\right)\ddot{\boldsymbol{\theta}} + \mathbf{J}_p\mathbf{C}(\boldsymbol{\theta}, \dot{\boldsymbol{\theta}})\dot{\boldsymbol{\theta}} + \mathbf{B}\dot{\boldsymbol{\theta}} = \bar{\mathbf{u}}, \tag{9}$$

where $\mathbf{I}$ is identity matrix. Unlike the manipulator dynamics in the case without joint torque feedback, the inertia matrix in (9) is not symmetric. Moreover, the vector $\mathbf{C}(\boldsymbol{\theta}, \dot{\boldsymbol{\theta}})\dot{\boldsymbol{\theta}}$ includes only coriolis accelerations, without centrifugal terms. $\mathbf{C}(\boldsymbol{\theta}, \dot{\boldsymbol{\theta}})$ is also not skew symmetric.

It is important to note that, due to the use of joint torque compensation in the control input, the relevant dynamics remaining to be computed are vastly simplified, when compared with the full robot link dynamics in the *computed torque method* without positive torque feedback [2, 5]. In addition, the computation (9) requires only knowledge of the polar rotor inertias and joint friction, eliminating the need to know all the link parameters as well. Nevertheless, in general, (9) is nonlinear in $\boldsymbol{\theta}$ due to $\mathbf{D}(\boldsymbol{\theta})$ which changes the inertia of the system and introduces coriolis terms caused by the rotors' movement in Cartesian space.

3 Control

3.1 Linear Rotor Dynamics

We will show now that for a large class of practical direct-drive robots, the system dynamics (9) are actually linear.

Proposition 1: A two DOF revolute robot with perpendicular axes is the only kinematic configuration with decoupled and linear rotor dynamics.

Proof: Given that both $\mathbf{J}_p$ and $\mathbf{B}$ in (9) are constant diagonal matrices, and $\mathbf{D}$ in (5) is upper triangular, for the system of equations to be decoupled requires $\mathbf{D}$ to be a zero matrix. For the first diagonal to be zero requires that all successive joint axes be perpendicular, $\alpha_i = \pm\pi/2$ for all twist angles $i = 1, \ldots, n-1$. Now, the first element of the second diagonal is,

$$\hat{z}_1^3(\boldsymbol{\theta}) = -c\theta_3 s\alpha_1 s\alpha_2 + c\alpha_1 c\alpha_2 = -c\theta_3,$$

which cannot be set to zero. Therefore a contradiction arises for $n > 2$.

□

It is clear from (5) that single and double link robots always have invariant $\mathbf{D}$ matrices. Now, the natural question is which kinematic configurations have invariant $\mathbf{D}$ matrices resulting in linear rotor dynamics.

Theorem 1: For an n-DOF revolute joint robot (n>2), the configuration matrix $\mathbf{D}(\boldsymbol{\theta})$ in (5) is independent of joint angles $\boldsymbol{\theta}$ iff there exist at least $n-2$ adjacent parallel joint axes. In this case the $\mathbf{D}$ matrix is

$$\mathbf{D} = \begin{bmatrix} 0 & c\alpha_1 & c\alpha_1 c\alpha_2 & \cdots & \prod_{j=1}^{n-1} c\alpha_j \\ 0 & 0 & c\alpha_2 & \cdots & \prod_{j=2}^{n-1} c\alpha_j \\ \vdots & \vdots & \vdots & \vdots & \vdots \\ 0 & 0 & 0 & \cdots & c\alpha_{n-1} \\ 0 & 0 & 0 & \cdots & 0 \end{bmatrix}. \quad (10)$$

Proof: We will prove the theorem by induction.
Step 1: For $n=3$ the nonzero terms in $\mathbf{D}_{(3\times 3)}$ are

$$\hat{z}_1^2 = c\alpha_1; \quad \hat{z}_2^3 = c\alpha_2$$

$$\hat{z}_1^3(\boldsymbol{\theta}) = -c\theta_3 s\alpha_1 s\alpha_2 + c\alpha_1 c\alpha_2$$

Either $\alpha_1 = 0$ or $\alpha_2 = 0$, or both; this annihilates the first term in $\hat{z}_1^3$ above. Hence theorem 1 holds for $n = 3$.
Step 2: Assume the statement is true for an m-DOF robot. Then for an $(m+1)$-DOF robot

$$\begin{aligned} \hat{z}_k^{m+1} &= [\mathbf{R}_m^{m+1}\mathbf{R}_k^m]_{(3,3)} \quad (11) \\ &= -s\alpha_m[\mathbf{R}_k^m(\boldsymbol{\theta})]_{(2,3)} + c\alpha_m[\mathbf{R}_k^m]_{(3,3)}. \end{aligned}$$

The m-DOF robot can have only $m-1$ or $m-2$ parallel axes according to theorem 1. In the first case the m-DOF robot must be planar and $[\mathbf{R}_k^m(\boldsymbol{\theta})]_{(2,3)} = 0 \quad \forall k \in \{1, ..., m\}$ (note that the last column in the transformation matrix is $[0,0,1]^T$ for a planar robot). In the second case, α_m must be zero to eliminate the $\boldsymbol{\theta}-$dependent term in (5). Therefore, in any case, at least one more parallel joint axis, i.e. $m-1$, for the $(m+1)$-DOF robot is required for an invariant $\mathbf{D}$,

$$\hat{z}_k^{m+1} = c\alpha_m \prod_{j=k}^{m-1} c\alpha_j = \prod_{j=k}^{m} c\alpha_j. \quad (12)$$

The steps (1) and (2) complete the proof.

□

The linear rigid body rotor dynamics (9) for an invariant $\mathbf{D}$ matrix are

$$\mathbf{J}_p(\mathbf{I} + \mathbf{D}^T)\ddot{\boldsymbol{\theta}} + \mathbf{B}\dot{\boldsymbol{\theta}} = \bar{\mathbf{u}}. \quad (13)$$

The result of the forgoing argument is a very useful and comprehensive tool to design robot controllers, since it permits recourse to a vast literature on the control of linear MIMO plants. Even a simple PD controller

$$\bar{\mathbf{u}} = -\mathbf{K}_p(\boldsymbol{\theta} - \boldsymbol{\theta}_d) - \mathbf{K}_v(\dot{\boldsymbol{\theta}} - \dot{\boldsymbol{\theta}}_d)$$

suffices to stabilize the manipulator. $\mathbf{K}_p$ and $\mathbf{K}_v$ are positive definite position and velocity gain matrices which are not symmetric or diagonal in general, due to the coupled dynamics of the plant. $\boldsymbol{\theta_d}$ and $\dot{\boldsymbol{\theta}}_d$ are the desired vectors of joint position and velocity. Critically damped responses can be achieved independent of the arm configuration.

For practical relevance it is important to point out the conditions of Theorem 1 are not very restrictive, since typically only the first three or four robot joints are directly actuated. Indeed, most industrial direct drive robots, including SCARA arms and anthropomorphic robots [14, 10] fall into this category.

3.2 General Three DOF Robots

Differential equation (9), which is mainly based on rotor dynamics, describes the motion of the robot with internal joint torque feedback. This dynamical system, in general, is a multi-input nonlinear system for robots that have more than two DOF. We showed that linear robot dynamics is also possible for multi-DOF robots under a fairly mild conditions, yet nonlinear rotor dynamics is substantially less complex than robot link dynamics. In this section we derive the rotor equation of motion for a general three DOF robot, where the viscous friction is eliminated for simplicity. Choosing three DOF is relevant from a practical point of view, because direct drive actuation is usually used for positioning the end effector in task space which can be accomplished by three joints.

It is desirable to change the parameters of the system as, $a_1 = c\alpha_1$ and $a_2 = c\alpha_2$. After substituting

$$\begin{aligned} a_3 &= a_1 a_2 \quad (14) \\ a_4 &= s\alpha_1 s\alpha_2 = (1 + 2a_1^2 a_2^2 - a_1^2 - a_2^2)^{1/2} \\ a_5 &= a_1 a_2 - a_4, \end{aligned}$$

in (5) and then in (9), one can derive the equations of motion of the robot,

$$\ddot{\theta}_1 = J_1^{-1}\bar{u}_1 \quad (15)$$

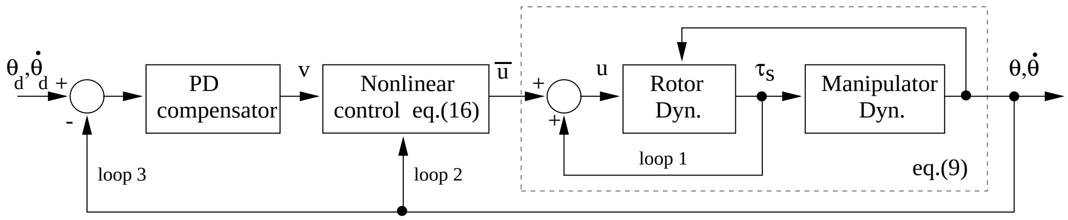

Figure 2: Architecture of the control system with positive joint torque feedback.

$$
\begin{aligned}
\ddot{\theta}_2 &= -a_2 J_1^{-1}\bar{u}_1 + J_2^{-1}\bar{u}_2 \\
\ddot{\theta}_3 &= (a_5 - a_4\, c\theta_3)J_1^{-1}\bar{u}_1 - a_2 J_2^{-1}\bar{u}_2 + J_3^{-1}\bar{u}_3 \\
&\quad -a_4\dot{\theta}_1\dot{\theta}_2 s\theta_3.
\end{aligned}
$$

A comparison of a these dynamical equations with those of a three DOF robot without joint torque feedback shows an essential simplification. The number of independent parameters which are relevant to the above equation is only five, including the polar inertias of the rotors and the cosine of the twist angles. Since $\boldsymbol{D}(\boldsymbol{\theta})$ is a triangular matrix, one can conclude that the proximal joint of a higher DOF robot has the same equation as (9). The reason is that the movement of proximal joints affects the motion of distal joints while, conversely, all dynamical effects of distal joints on the proximal ones are totally compensated by the torque sensor signals. As is the case for link dynamics, the rotor dynamics (15) can be linearized by feedback linearization [15] or equivalently inverse dynamics. The nonlinear input transformation $\mathbf{v} = \boldsymbol{\beta}(\boldsymbol{\theta},\dot{\boldsymbol{\theta}})\bar{\mathbf{u}} + \boldsymbol{\Gamma}(\boldsymbol{\theta},\dot{\boldsymbol{\theta}})$ by feedback linearization can linearize and also decouple the nonlinear system. One can inspect that by taking the right hand side of (15) as the new inputs v_i, the control problem reduces trivially to control three double integrator systems,

$$\ddot{\theta}_i = v_i \qquad i = 1,2,3.$$

A linear control law with respect to the new inputs v_i can be easily designed for trajectory tracking or set-point regulation. The link between the old and new inputs is provided by $\bar{\mathbf{u}} = \boldsymbol{\beta}^{-1}(\boldsymbol{\theta},\dot{\boldsymbol{\theta}})[\mathbf{v} - \boldsymbol{\Gamma}(\boldsymbol{\theta},\dot{\boldsymbol{\theta}})]$,

$$
\begin{aligned}
\bar{u}_1 &= J_1 v_1 \qquad\qquad (16)\\
\bar{u}_2 &= a_1 J_2 v_1 + J_2 v_2 \\
\bar{u}_3 &= (a_3 - a_4 c\theta_3)J_3 v_1 + a_2 J_3 v_2 + J_3 v_3 \\
&\quad + J_3 a_4 \dot{\theta}_1\dot{\theta}_2 s\theta_3.
\end{aligned}
$$

Fig. 2 illustrates the structure of the overall controller which consists of three feedback loops. The innermost loop is joint torque feedback which totally compensates the link dynamics and the interaction of the robot with its environment. The second feedback linearizes the rotor dynamics. Obviously, this loop is not needed if the rotor dynamics are already linear. Finally, the outer loop provides position and velocity feedback for the linearized system.

4 Design Considerations

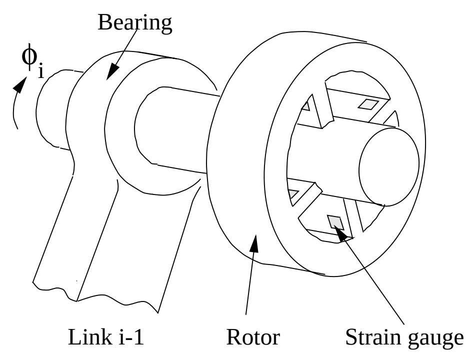

Figure 3: Integrated sensor and rotor can compensate joint friction.

Stiction, dry friction and the torque caused by the supply wires which pass from one joint to the next are a source of joint torque nonlinearity in practice. Special care in the design stage should be given such that all these torques are observable by the sensors, otherwise they enter as disturbances to the control system which degrades the performance. In this regard bearing configuration and the sensor location play the key roles. As an example, the rotor can be mounted by some sprocket, on which strain gauges are cemented, to its shaft, Fig. 3. Such a arrangement can potentially compensate joint friction as well as link dynamics, and leaves neatly the pure inertial dynamics of the rotors as the plant dynamics.

5 Conclusion

The equations of motion of direct drive robots with positive joint torque feedback have been derived. The conditions on the kinematic structure of the robot to possess linear dynamics have been presented. The resulting rotor dynamics are determined solely by the polar inertia of motor rotors and joint twist angles, which can be identified precisely in practice. For the linear dynamics, a centralised PD controller can be designed for accurate and high bandwidth control, while in the nonlinear case feedback linearization is applicable. We showed that the number of terms in the equations of motion is significantly less than of the links. The system parameters are only the polar inertias of the rotors and the twist angles. To this end, it worth pointing out that, although the positive joint torque feedback begun in the field of robot motion control, it can be envisaged in other robotic applications such as force and impedance control. In particular, in teleoperation the link dynamics can be effectively compensated by this method to achieve high fidelity force reflection.

Acknowledgements

This project was supported by the PRECARN TDS Project, through MPB Technologies of Montreal, Quebec.

References

[1] F. Aghili, M. Buehler, and J. M. Hollerbach. A new indirect adaptive control strategy for a synchronous direct drive motor. In *Proc. IEEE Int. Conf. Robotics and Automation*, pages 2865–2870, Minneapolis, MN, Apr 1996.

[2] C. H. An, C. G. Atkeson, and J. M. Hollerbach. *Model-Based Control of a Robot Manipulator.* MIT Press, Cambridge, MA, 1988.

[3] H. Asada and K. Youcef-Toumi. *Direct-Drive Robots.* MIT Press, London, 1987.

[4] D. Chen and B. Paden. Adaptive linearization of hybrid step motors: stability analysis. *IEEE Trans. Automatic Control*, 38(6):874–887, June 1993.

[5] J.J. Craig. *Introduction to Robotics Mechanics and Control.* Addison Wesley, Reading, MA, 1986.

[6] F. Filicori, C. G. Lo Bianco, and A. Tonielli. Modeling and control strategies for a variable reluctance direct-drive motor. *IEEE Trans. Industrial Electronics*, 40(1):105–115, 1993.

[7] E. Freund. Fast nonlinear control with arbitrary pole placement for industrial robots and manipulators. *Int. J. Robotics Research*, 1(1), 1993.

[8] M. Hashimoto. Robot motion control based on joint torque sensing. In *Proc. IEEE Int. Conf. Robotics and Automation*, pages 256–1261, 1989.

[9] J. Hollerbach, I. Hunter, J. Lang, S. Umans, and R. Sepe. The McGill/MIT Direct Drive Motor Project. In *Proc. IEEE Int. Conf. Robotics and Automation*, pages 611–617, May 1993.

[10] V. Daniel Hunt. *Understanding Robotics.* Academic Press, San Diego, CA, 1990.

[11] K. Kosuge, H. Takeuchi, and K. Furuta. Motion control of a robot arm using joint torque sensors. *IEEE Trans. Robotics and Automation*, 6(2):258–263, 1990.

[12] J. Y. S. Luh, M. W. Walker, and R. P. Paul. Resolved acceleration control of mechanical manipulators. *IEEE Trans. Automatic Control*, AC-25, 1980.

[13] D. G. Manzar, M. Varghese, and J. S. Thorp. Variable reluctance motor characterization. *IEEE Trans. Industrial Electronics*, 36(1):56–63, 1989.

[14] B. Powell. Direct drives for precision robots. *Machine Design*, pages 49–51, Mar 1986.

[15] M. W. Spong and M. Vidyasagar. *Robot Dynamics And Control.* John Wiley & Sons, New York, 1989.

[16] D. G. Taylor. Nonlinear control of electric machines: An overview. *IEEE Control System*, December:41–51, 1994.

[17] R. S. Wallace and D. G. Taylor. Low-torque-ripple switched reluctance motors for direct-drive robotics. *IEEE Trans. Robotics and Automation*, 7(6):733–742, 1991.

[18] L. Whitcomb, A. Rizzi, and D. Koditschek. Comparative experiments with a new adaptive controller for robot arms. *IEEE Trans. Robotics and Automation*, 9(1):59–70, Feb 1993.